ELSEVIER

Contents lists available at ScienceDirect

Precision Engineering

journal homepage: www.elsevier.com/locate/precision



Check for updates

Evaluating the standard uncertainty due to the voxel size in dimensional computed tomography

Joseph John Lifton

Advanced Remanufacturing and Technology Centre, 3 CleanTech Loop, 01-01, CleanTech Two, 637143, Singapore

ABSTRACT

X-ray computed tomography (XCT) is a promising tool for making dimensional measurements of complex engineering components. The adoption of XCT as a measurement tool is hindered by the inability to evaluate the uncertainty of XCT-based dimensional measurements; simply put, XCT users cannot specify how good (or bad) their measurements are. In this work, equations and a method are given to evaluate the standard uncertainty due to the voxel size; this being one of several sources of uncertainty in XCT-based dimensional measurements. It is envisioned that this standard uncertainty component will be combined with other standard uncertainties in a task-specific uncertainty budget, thus providing end users with a statement of XCT measurement uncertainty. It is claimed here that evaluating the standard uncertainty of the voxel size by means of a calibrated length leads to a traceable voxel size. For the example considered in this work, the voxel size is evaluated to be 80.005 μ m \pm 0.001 μ m, with the voxel size uncertainty expressed as one standard deviation. When the standard uncertainty of the voxel size is propagated through to the final measurement result of a machined aluminium length bar, the standard uncertainty due to the voxel size is evaluated as \pm 1.01 μ m for a bi-directional length of nominally 55 mm.

1. Introduction

X-ray computed tomography (XCT) is increasingly being used for dimensional metrology by manufacturing industries, particularly for the measurement of polymer and low-density metallic parts. This increased uptake of the technology is due to manufacturing industries becoming more aware of what XCT has to offer over and above traditional tactile and optical instruments, namely the ability to non-destructively measure the internal and external geometry of an object with micron-level resolution in a single pass. Another emerging application of XCT is the measurement and inspection of additively manufactured components, which often have complex internal features that cannot be measured non-destructively using any other technique [1].

Although XCT offers a number of benefits over traditional measurement instruments, there are still a number of factors that are stifling the uptake of the technology. These include: high purchase and maintenance costs, long measurement times, lack of standardisation, and the inability to evaluate the uncertainty of XCT measurements, where uncertainty is the doubt associated with a measurement result; this work is concerned with the latter point. Presently there are no widely accepted approaches to evaluate the task-specific uncertainty of XCT-based measurements, meaning that end users and service providers do not know how good (or bad) their dimensional measurements are.

The ISO 10360-11 standard on acceptance and reverification tests for XCT systems is still under development [2] but offers to provide some

rigor and standardisation to the field. The ISO 10360-11 standard will allow XCT system developers to specify the measurement performance of their systems under well-defined conditions [3] and allow end users to routinely check that their system is still in specification. Such a standard is a very welcome development, but it does not solve the problem of evaluating the task-specific uncertainty of an XCT-based dimensional measurement.

The evaluation of task-specific measurement uncertainty by means of XCT simulation is an active area of research [4]. The idea is to repeatedly simulate an XCT scan of an object and to perturbate sources of uncertainty in the simulation based on predefined statistical distributions. The main advantage of this approach is that influence factors can be isolated and studied in detail, this is impossible to do experimentally. There are a number of disadvantages to an entirely simulation-based approach. Firstly, XCT simulations are slow, it often takes longer to simulate a CT scan then it does to conduct a scan experimentally. This limitation could be overcome by using high-end computational hardware, or the development of faster simulation tools. Secondly, information concerning the statistical distributions of influence factors needs to be known before simulation. Many influence factors are scan-dependent and may need to be evaluated on a case-by-case basis, for example, the focal spot drift of an X-ray tube operated at maximum power will differ from that of a tube operated at low power. Thirdly, methods for theoretically or experimentally evaluating the distributions of these influence factors still need to be developed, the nature of many influence factors is poorly

E-mail address: Lifton_Joseph_John@artc.a-star.edu.sg.

understood (this applies to the current work as well). Fourthly, XCT simulation tools require significant tuning in order for the simulated data to match the data produced by the physical system, as demonstrated by Hiller et al. [5]. XCT simulation tools are invaluable to the study of XCT measurement uncertainty, however, simulation may not be the solution to evaluating XCT measurement uncertainty in and of itself.

The substitution method is another approach for evaluating task-specific uncertainty of XCT measurements [6]. The idea is to measure a calibrated sample in the same manner as the considered workpiece; the dimensions of the calibrated sample enable the measurement bias to be evaluated, alongside other sources of uncertainty such as: measurement repeatability, thermal expansion and deviations in form, surface texture and expansion coefficients. Based on the assumption that the calibrated sample and the considered workpiece are sufficiently similar, the measurement uncertainty of the calibrated sample can be transferred to the considered workpiece. The challenge here is developing calibrated samples that are sufficiently representative of the considered workpiece [7]; this seems like an exhausting task due to the range of possible component geometries, surface textures and materials found in manufactured goods.

In our previous work [8], we suggested that a series of simple tests be developed to evaluate prominent sources of uncertainty in XCT measurements. We proceeded to develop a simple method for evaluating the standard uncertainty due to the surface determination process, $u_{L\ SD}$, where surface determination is the process of defining a surface from an XCT data-set and is regarded as a prominent source of uncertainty in XCT-based measurements [9]. In the present work we build upon our previous work and offer a simple method to evaluate the standard uncertainty due to the voxel size, $u_{L\ Sv}$, which can be combined with $u_{L\ SD}$ and other standard uncertainties to yield the combined standard uncertainty, $u_{L\ C}$ as follows:

$$u_{Lc} = \sqrt{u_{LSD}^2 + u_{LS_v}^2 + u_{LGM}^2 + u_{LSR}^2 + u_{LT}^2 + u_{LR}^2},$$
 (1)

where $u_{L\ GM},\ u_{L\ SR},\ u_{L\ T}$ and $u_{L\ R}$ are the standard uncertainties due to geometric misalignment, structural resolution, temperature and measurement repeatability, respectively. The subscript L in equation (1) is used to denote the influence of these standard uncertainties for an XCT-based length measurement, but the concept could be extended to any other XCT-based dimensional measurement. The uncertainty budget given in equation (1) is not claimed to be exhaustive, it is intended as an illustration of what a task-specific uncertainty budget may look like. The key idea is that an uncertainty budget like this can be formed for an arbitrary object and is not reliant on Monte-Carlo simulations or the substitution of a similar calibrated workpiece [10].

The uncertainty of the voxel size is considered in this work because it has the potential to be a predominant source of uncertainty in XCTbased dimensional measurements. A voxel is a volume-element, a 3D version of a 2D picture element, a pixel. XCT data can be thought of as a 3D image composed of voxels, with each voxel containing a grey value describing the local X-ray attenuation of the scanned object. When we make dimensional measurements from an XCT volume we are in fact measuring in units of voxels. We use the physical geometry of the XCT system and the detector pixel size to calculate the voxel size in units of millimeters. A measurement result is therefore converted from units of voxels to units of millimeters by multiplying by the voxel size: note that this is done automatically by XCT data-processing software but is stated here for completeness. Since the voxel size is a derived value, there is an uncertainty associated with it. The purpose of this work is to develop a simple method to determine the uncertainty of the voxel size and to propagate it though to the final result of an arbitrary XCT measurement, such that more comprehensive task-specific uncertainty budgets can be built, ultimately leading to a greater confidence in XCT-based measurements.

2. Method

The methodology adopted in this work is as follows: equations are first derived to propagate the uncertainty of the voxel size through an XCT-based measurement (Section 2.1); next, the voxel size uncertainty is determined experimentally (Section 2.2); the determined voxel size uncertainty is then used to evaluate the standard uncertainty due to the voxel size for the measurement of an arbitrary object (Section 2.3).

2.1. Derivation and propagation of the voxel size uncertainty

The voxel size, S_{ν} , is normally automatically calculated by an XCT system based on the detector pixel size, S_p and the geometric magnification, M, of the scan:

$$S_{v} = \frac{S_{p}}{M}.$$
 (2)

The geometric magnification of a scan is calculated based on the distance between the X-ray focal spot position and the rotation axis of the sample manipulator, $L_{\rm SOD}$, alongside the distance between the X-ray focal spot and the imaging plane of the X-ray detector, $L_{\rm SDD}$:

$$M = \frac{L_{\text{SDD}}}{L_{\text{SOD}}}.$$
 (3)

Determining S_{ν} in this manner is subject to uncertainties in S_p , $L_{\rm SOD}$ and $L_{\rm SDD}$. It is nontrivial to calibrate these terms, particularly $L_{\rm SOD}$ and $L_{\rm SDD}$, as doing so may require interferometers and other specialist equipment that is not available to end users.

A simpler approach to calculating the voxel size is used in this work that relies on measuring a single calibrated length, L_{cal} via XCT:

$$S_{v} = \frac{L_{\text{cal}}}{N_{v}},\tag{4}$$

where N_{ν} is the length measured via XCT in units of voxels.

Using the law of propagation of uncertainty, the standard uncertainty of the voxel size u_{S_v} is calculated as:

$$u_{S_{\nu}} = \sqrt{\left(\frac{\partial S_{\nu}}{\partial L_{\text{cal}}}\right)^{2} u_{L_{\text{cal}}}^{2} + \left(\frac{\partial S_{\nu}}{\partial N_{\nu}}\right)^{2} u_{N_{\nu}}^{2}} \tag{5}$$

where $u_{L_{\rm val}}$ is the uncertainty of the calibrated length, $u_{N_{\nu}}$ is the uncertainty of the length measured via XCT in units of voxels and the partial derivatives are:

$$\frac{\partial S_{v}}{\partial L} = \frac{1}{N} \tag{6}$$

$$\frac{\partial S_{\nu}}{\partial N_{\nu}} = -\frac{L_{\text{cal}}}{N_{\nu}^2}.\tag{7}$$

Let us propagate u_{S_v} through an arbitrary XCT measurement of length L, to do so we must express L as:

$$L = N_{vL} \times S_v \tag{8}$$

where N_{vL} is L measured in units of voxels and is treated as a constant. The uncertainty of L due to u_{S_v} is therefore:

$$u_{L S_{\nu}} = N_{\nu L} \times u_{S_{\nu}} \tag{9}$$

Equation (9) simply says that each voxel has an uncertainty to its size, so the uncertainty of the considered length is proportional to the length expressed in units of voxels.

It should be noted that the calibrated length $L_{\rm cal}$ used to determine $u_{S_{\nu}}$ should be XCT scanned at the same magnification and using the same scan settings as the object of interest and that the position of the rotation stage should not be moved between scans. Also, equations (8) and (9) are not limited to lengths, but can be applied for any dimensional

measurement, length is just used as a simple intuitive example.

2.2. Experimental determination of the voxel size uncertainty

To evaluate equation (5) we need the following terms: $L_{\rm cal}$, N_{ν} , $u_{L_{\rm cal}}$, and $u_{N_{\nu}}$. For $L_{\rm cal}$ and $u_{L_{\rm cal}}$ we use a calibrated ball bar made with two ruby spheres mounted on carbon fibre rods, see Fig. 1. The centre-to-centre distance of the ball bar has been calibrated by the National Metrology Centre of Singapore, thus providing traceability to the metre. The calibrated length, $L_{\rm cal}$, is 59.9938 mm, the standard uncertainty of the calibrated length, $u_{L_{\rm cal}}$, is 0.9 µm. The standard uncertainty due to the thermal expansion of the calibrated length is also evaluated, u_T , which includes the uncertainty due to the change in temperature in the XCT scanner, the uncertainty due to the accuracy of the thermometer and the uncertainty due to the thermal expansion coefficients of the calibrated length bar. Thus we substitute $u_{L_{\rm cal}}'$ for $u_{L_{\rm cal}}$ in equation (5), where $u_{L_{\rm cal}}'$ is calculated as:

$$u'_{L_{cal}} = \sqrt{u_{L_{cal}}^2 + u_T^2} \tag{10}$$

Determining N_{ν} and $u_{N_{\nu}}$ requires the ball bar to be XCT scanned and the uncertainty of the XCT-based length measurement to be evaluated in units of voxels. To achieve this, it is assumed that measuring the ball-bar under all possible 'sensible' scan conditions is sufficient to capture the uncertainty of the XCT scan process. By 'sensible' we mean scan conditions that are deemed viable by a trained XCT system operator, and that are not obviously detrimental to the quality of the scan. We expect this approach to lead to a larger measurement variation than simply repeatedly scanning the length bar using the same scan settings. The approach adopted is designed to capture the measurement repeatability alongside the influence of each scan setting. By simply repeatedly scanning the length bar using the same scan settings there is a risk that u_{N_v} may be underestimated. An experiment is therefore deigned to perturbate all possible scan conditions of the ball bar. These conditions are specified in Table 1 alongside the resulting ball bar length measurement in units of voxels. The terms N_v and u_{N_v} are calculated as the mean and standard deviation of the ball bar length measurements, respectively. The shape of the ball bar length distribution is unknown; therefore it is assumed to be rectangular for safety reasons [11]. The standard deviation u_{N_v} is calculated as $a/\sqrt{3}$ where a is half the range of the ball bar length measurements.

This gives us all the information required to evaluate equation (5), doing so gives the value of $u_{S_{\nu}}$ to be 0.001 μ m, a surprisingly small value indeed, but bear in mind that this is the uncertainty of the size of a single voxel. The calibrated voxel size, S_{ν} from equation (4) is calculated as 80.005 μ m, thus the voxel size uncertainty is approximately 0.002% of the voxel size

The time taken to conduct each scan in Table 1 is approximately 30 min. The total time taken to run the experiment in Table 1 is

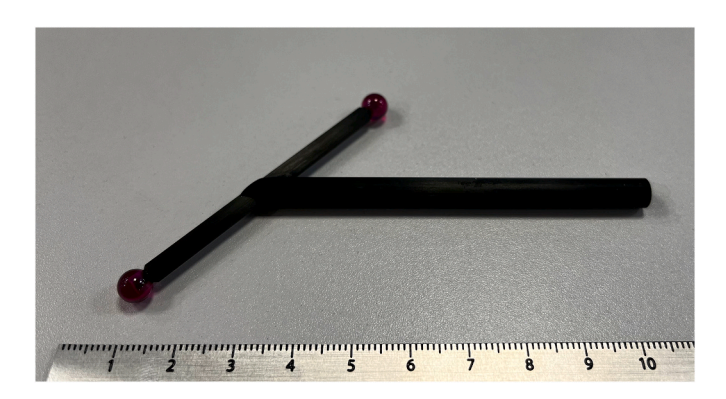


Fig. 1. A calibrated ball bar composed of two ruby spheres mounted on carbon fibre rods is used to evaluate the uncertainty of the voxel size, u_{S_v} .

approximately 7.5 h. All scans are conducted using a Nikon XT H 225 XCT cone-beam CT system (Nikon X-tek Systems Ltd., UK) with the sample being rotated through a full 360°. Reconstruction is performed using Nikon's CT Pro software which uses an equiangular Feldkamp, Davis, and Kress algorithm [12]. All data processing is undertaken in Volume Graphics VGSTUDIO MAX 3.4 (Volume Graphics GmbH, Heidelberg, Germany). The surface of the sample is determined in VGSTUDIO MAX using the advanced method with the default settings. Spheres are fitted to the surface of each ruby sphere using the least-squares method and the Euclidean distance between the centres of the fitted spheres is calculated.

The next step is to propagate the voxel size uncertainty through the measurement of an arbitrary object, this is considered in the next subsection.

2.3. Evaluating the standard uncertainty due to the voxel size for an arbitrary object

The object used to demonstrate the developed method is a machined aluminium length bar that presents both uni- and bi-directional lengths, see Fig. 2. The bi-directional lengths range from 5 to 55 mm in steps of 10 mm, the uni-directional lengths range from 10 to 50 mm in steps of 10 mm

With reference to Fig. 2, the uni- and bi-directional lengths are formed by intersection points between a line (datum D) and least-squares planes fitted to the face of each step of the length bar. Line D is formed by creating a midplane between the side planes B and C and intersecting it with the top plane A, then translating the intersection line by -2.5 mm in the z direction from plane A.

The length bar is XCT scanned using the nominal settings defined in the first row of Table 1 and the data processing settings described in the previous section. The dimensions of the length bar are evaluated in units of voxels and then multiplied by the calibrated voxel size, S_{ν} as per equation (8). The uncertainty of the lengths due to the voxel size uncertainty is calculated as per equation (9).

Reference measurements of the length bar are made by means of a coordinate measuring machine (CMM) in order to compare the magnitude of the standard uncertainty due to the voxel size to the XCT measurement error. The XCT measurement error is calculated as XCT measurements minus the CMM measurements. It should be noted that the CMM reference measurements are not used to evaluate the standard uncertainty due to the voxel size and are not required to implement the proposed method, they are simply included to provide an additional comparison for the interested reader.

The dimensions of the length bar are measured using a Zeiss Accura II (Carl Zeiss AG, Germany) CMM, using a 3 mm diameter diamond probe with a 200 mN probing force. All planes are scanned using a 6 mm/s scanning speed. Traceability of the CMM length measurements is achieved using calibrated ceramic gauge blocks. The uncertainty of the CMM measurements is evaluated using the non-substitution method described in Ref. [13]. The expanded uncertainty with a coverage factor of k=2 for a confidence probability of approximately 95% does not exceed $\pm 3~\mu m$ for all the lengths of the length bar.

3. Results

The XCT-based uni- and bi-directional length measurements of the aluminium length bar are listed in Table 2 in units of voxels and in millimeters, alongside the respective standard uncertainty due to the voxel size. Obviously, the uncertainty due to the voxel size is larger for longer lengths and is not affected by a length being uni- or bi-directional. For all the lengths considered in this example, the standard uncertainty due to the voxel size is in the order of 1 μ m or less; this is due to the uncertainty of the voxel size, u_{S_r} , being low in the first place. A low value of u_{S_r} can be achieved by using a calibrated length with a low calibration uncertainty, $u_{L_{val}}$, also by maximising the number of voxels the calibrated

Table 1 X-ray CT scan settings varied to determine N_v and u_{N_v} .

Voltage (kV)	Current (µA)	Exposure time (s)	Copper X-ray filter thickness (mm)	Number of projections	Projection averages	Object orientation	Length in voxels
200	200	2	0.5	400	2	Diagonal	749.885
220	200	2	0.5	400	2	Diagonal	749.875
180	200	2	0.5	400	2	Diagonal	749.878
200	220	2	0.5	400	2	Diagonal	749.880
200	180	2	0.5	400	2	Diagonal	749.889
200	200	2.83	0.5	400	2	Diagonal	749.879
200	200	1.42	0.5	400	2	Diagonal	749.883
200	200	2	0.75	400	2	Diagonal	749.869
200	200	2	0.25	400	2	Diagonal	749.877
200	200	2	0.5	440	2	Diagonal	749.877
200	200	2	0.5	360	2	Diagonal	749.885
200	200	2	0.5	400	4	Diagonal	749.892
200	200	2	0.5	400	1	Diagonal	749.866
200	200	2	0.5	400	2	Vertical	749.865
200	200	2	0.5	400	2	Horizontal	749.881
-						Mean, N_{ν} Standard Deviation,	749.879 0.008
						$u_{N_{\nu}}$	

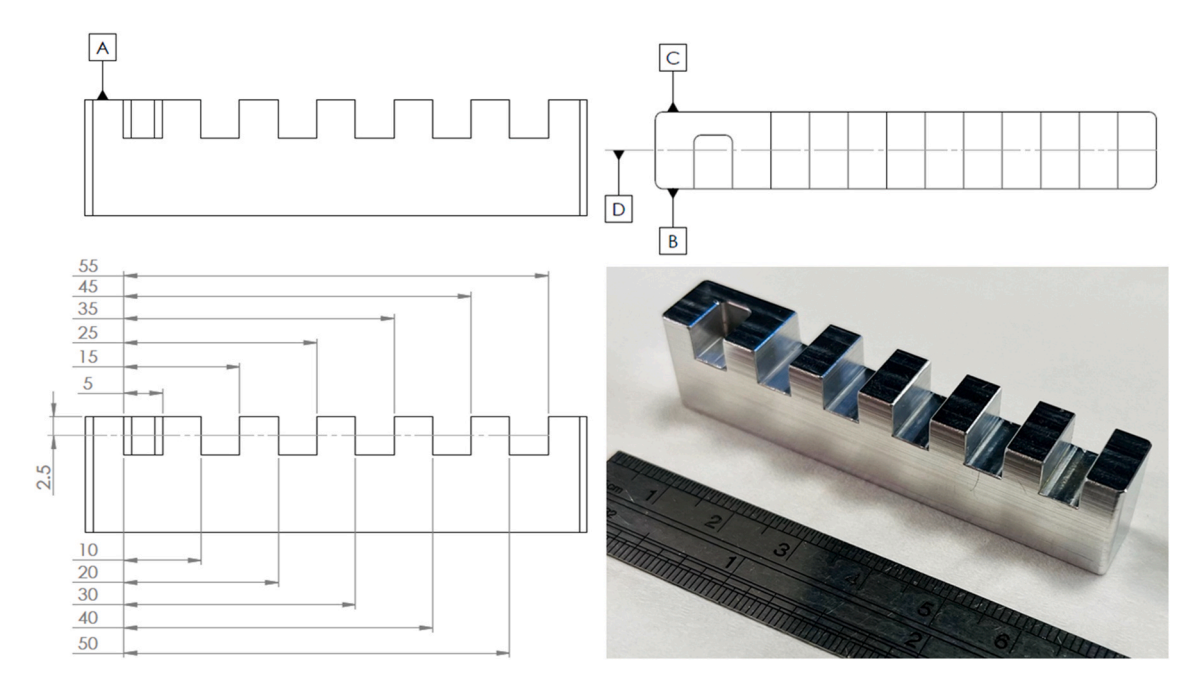


Fig. 2. A machined aluminium length bar that presents both uni- and bi-directional lengths. Datum A is a plane fitted to the top surface of the length bar. Datum B and C are planes fitted to the sides of the length bar. Datum D is a line based on intersecting the midplane of B and C with A and translating it -2.5 mm in z from datum A.

Table 2 Results for propagating the uncertainty due to the voxel size for an arbitrary object. The terms L, N_{vL} , and u_{LS_v} are from equations (8) and (9) respectively.

Length Type	Measured length, N_{vL} (voxels)	Measured length, L (mm)	Standard uncertainty due to the voxel size, $u_{L S_{\nu}}$ (µm)	Measurement error XCT – CMM (μm)
Bi-directional	62.407	4.993	0.09	-5.16
	187.405	14.993	0.28	-4.70
	312.384	24.992	0.46	-5.81
	437.380	34.992	0.64	-5.54
	562.401	44.995	0.83	-3.28
	687.424	54.997	1.01	0.10
Uni-directional	124.994	10.000	0.18	0.12
	249.974	19.999	0.37	-0.88
	374.969	29.999	0.55	-0.74
	499.960	39.999	0.74	-0.88
	624.964	50.000	0.92	0.06

length spans, N_{ν} , and minimising the value of $u_{N_{\nu}}$. The latter will depend on the metrological quality of the XCT system being used (low drift, good geometric alignment, etc.).

The error of the XCT length measurements, with respect to the reference CMM measurements, is given in Table 2. The measurement error for the uni-directional lengths is within the uncertainty of the CMM measurement uncertainty, whilst the measurement error for the bidirectional lengths mostly exceeds the CMM measurement uncertainty; this is more easily understood by plotting the measurement error as a function of length and dimension type, as shown in Fig. 3. This result indicates that there is some degree of systematic error in the bidirectional length measurements, this is most likely caused by the surface determination algorithm, which is well-known to influence bidirectional lengths to a greater degree than uni-directional lengths [14]. This behavior is seen because the two surfaces that form a bi-directional length move in opposing directions when the surface extraction parameters are changed, causing the length to increase or decrease. Whilst the two surfaces that form an uni-directional length move in the same direction when the surface extraction parameters are changed; see Ref. [15] for a detailed study of this behavior. Thus, any slight error in the determined surface will lead to greater errors in bi-directional lengths than uni-directional lengths.

It is important to note that Fig. 3 does not suggest that the XCT-based uni-directional length measurements have a lower uncertainty than the CMM measurements, since the expanded uncertainty of the XCT measurements has not been evaluated. Only one component of the XCT measurement uncertainty has been evaluated in this work: the standard uncertainty due to the voxel size, which is indicated by the error bars in Fig. 3.

Fig. 3 also shows that there is no obvious trend between the XCT measurement error and the feature length; if the measurement error increased (or decreased) as length increased then this would indicate an error in the voxel size. Given that this trend is not present in the results we can be confident that the error of the voxel size has been successfully minimised.

4. Discussion and conclusions

Equations and a method for evaluating the standard uncertainty due to the voxel size have been described, and a worked example provided. The standard uncertainty due to the voxel size can be included in a task-specific uncertainty budget such as that illustrated in equation (1). The proposed method is simple to undertake and only requires access to a calibrated length, thus making the method suitable for researchers, engineers and service providers to adopt.

The most striking claim of this work is that, for the first time, a traceable voxel size has been achieved. In previous work, calibrated lengths have been used to determine the voxel size [16-18], however, none of these studies have gone so far as to evaluate the uncertainty of the voxel size, or to propagate the voxel size uncertainty through to the final measurement result, these being the main contributions of this work. It is important to note that the author is not claiming the final XCT measurement is traceable, only that the voxel size is traceable, and only under the considered scan conditions.

One disadvantage of the proposed method is the scan time required to experimentally determine $u_{N_{\nu}}$ and N_{ν} , this being approximately 7.5 h in the present work. This is a consequence of XCT scans being slow compared to the run time of an optical or tactile instrument (measurement set up times for XCT can however be faster than optical and tactile instruments). One strategy to reduce the total scan time is to reduce the number of scans required; this could be achieved by choosing to only vary scan parameters that have a comparatively large influence on the measurement result. A further study would be required to generalise what these scan parameters may be.

Another point to note is that, if the calibrated voxel size is found to be significantly different from the uncorrected voxel size, then recon-

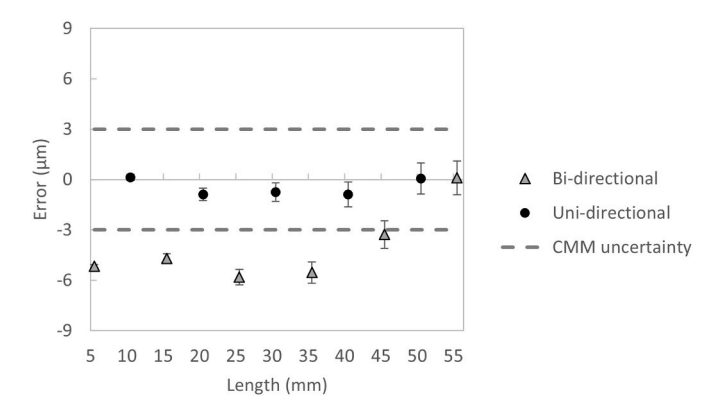


Fig. 3. A plot of XCT measurement error with respect to the reference CMM measurements for the aluminium length bar. Bi-directional and uni-direction lengths are plotted separately. The expanded uncertainty of the reference CMM measurements is also plotted for reference. The error bars represent the standard uncertainty due to the voxel size for each length measurement.

structing with the uncorrected voxel size may cause errors in the grey values of the reconstruction volume. That is to say that the filtered backprojection reconstruction algorithm relies on values of S_p , L_{SOD} and $L_{\rm SDD}$, and if these values are incorrect then the reconstruction quality will suffer [19]. We therefore suggest that the method proposed in this work is better suited to XCT systems that have undergone thorough geometric alignment, such that the values of S_p , $L_{\rm SOD}$ and $L_{\rm SDD}$ are not so erroneous as to cause reconstruction artifacts. The development of methods to estimate the geometric misalignment of an XCT system is an active topic of research, see Refs. [19-21]. Such methods could be used to estimate the values S_p , L_{SOD} and L_{SDD} and their respective uncertainties, these uncertainties could then be propagated through equations (2) and (3) to give the uncertainty of the voxel size, and the calibrated values of S_p , $L_{\rm SOD}$ and $L_{\rm SDD}$ used during reconstruction to avoid the aforementioned reconstruction artifacts. This approach will be considered in future work on evaluating the standard uncertainty due to the geometric misalignment of the XCT system.

The notion of task-specific uncertainty budgets for XCT-based dimensional measurements is very appealing, as it is able to accommodate the material dependence of XCT-based dimensional measurements. That is to say, if we were to measure two parts having the same geometry but one is made from steel and the other from aluminium, the quality of the XCT data would be far worse for the steel component than for the aluminium component due to the significantly higher density of steel, hence the measurement uncertainty of the steel component would be larger. A task-specific uncertainty budget has the flexibility to accommodate this material dependence, whereas a system-level statement of uncertainty, such as the maximum permissible error [22], would not easily be able to accommodate this material dependence, and would therefore lead to a potential overestimation of uncertainty for the aluminium component in the above example.

In future work, a worked example of a task-specific uncertainty budget will be presented. This will draw on the present work on evaluating the standard uncertainty of the voxel size, alongside our previous work on the standard uncertainty due to surface determination. Other standard uncertainties that can easily be considered are the measurement repeatability, thermal expansion of the workpiece, and sample orientation.

Declaration of competing interest

The authors declare that they have no known competing financial interests or personal relationships that could have appeared to influence the work reported in this paper.

Acknowledgements

This research is supported by A*STAR under its Industry Alignment Fund–Pre Positioning (IAF-PP), Grant number A20F9a0045. Any opinions, findings and conclusions or recommendations expressed in this material are those of the authors and do not reflect the views of the A*STAR.

References

- Dewulf W, Bosse H, Carmignato S, Leach R. Advances in the metrological traceability and performance of X-ray computed tomography. CIRP Ann 2022. https://doi.org/10.1016/j.cirp.2022.05.001.
- [2] ISO/DIS 10360-11 Geometrical product specifications (GPS) acceptance and reverification tests for coordinate measuring systems (CMS) - Part 11: CMSs using the principle of X-ray computed tomography (CT).
- [3] Zwanenburg EA, Williams MA, Warnett JM. Performance testing of dimensional X-ray computed tomography systems. Precis Eng 2022;77:179–93. https://doi.org/10.1016/j.precisioneng.2022.05.005.
- [4] Binder F, Bircher BA, Laquai R, Küng A, Bellon C, Meli F, et al. Methodologies for model parameterization of virtual CTs for measurement uncertainty estimation. Meas Sci Technol 2022;33(10). https://doi.org/10.1088/1361-6501/ac7b6a.
- [5] Hiller J, Reindl LM. A computer simulation platform for the estimation of measurement uncertainties in dimensional X-ray computed tomography. Measurement 2012;45(8):2166–82. https://doi.org/10.1016/j. measurement.2012.05.030.
- [6] Praniewicz M, Fox JC, Saldana C. Toward traceable XCT measurement of AM lattice structures: uncertainty in calibrated reference object measurement. Precis Eng 2022;77:194–204. https://doi.org/10.1016/j.precisioneng.2022.05.010.
- [7] BS EN ISO 15530-3. Geometrical product specifications-coordinate measuring machines: technique for determining the uncertainty of measurement, part 3: use of calibrated workpieces or measurement standards. 2011.
- [8] Lifton JJ, Liu T. Evaluation of the standard measurement uncertainty due to the ISO50 surface determination method for dimensional computed tomography. Precis Eng 2020;61:82–92. https://doi.org/10.1016/j.precisioneng.2019.10.004.
- [9] Yang X, Sun W, Giusca CL. An automated surface determination approach for computed tomography. NDT E Int 2022;131:102697. https://doi.org/10.1016/j. pdtpii/ 2022.105697

- [10] Ferrucci M, Ametova E. Charting the course towards dimensional measurement traceability by x-ray computed tomography. Meas Sci Technol 2021;32(9). https://doi.org/10.1088/1361-6501/abf058.
- [11] JCGM 100:2008 GUM 1995 with minor corrections, Evaluation of measurement data: guide to the expression of uncertainty in measurement. 2008.
- [12] Feldkamp LA, Davis LC, Kress JW. Practical cone-beam algorithm. J Opt Soc Am A 1984;1(6):612–9. https://doi.org/10.1364/JOSAA.1.000612.
- [13] Flack D. Good practice guide no. 130, co-ordinate measuring machine task-specific measurement uncertainties. UK: National Physical Laboratory; 2013.
- [14] Lifton JJ, Malcolm AA, McBride JW. A simulation-based study on the influence of beam hardening in X-ray computed tomography for dimensional metrology. J X Ray Sci Technol 2015;23(1):65–82. https://doi.org/10.3233/xst-140471.
- [15] Kiekens K, Welkenhuyzen F, Tan Y, Bleys P, Voet A, Kruth JP, et al. A test object with parallel grooves for calibration and accuracy assessment of industrial computed tomography (CT) metrology. Meas Sci Technol 2011;22(11). https://doi. org/10.1088/0957-0233/22/11/115502.
- [16] Müller P, Hiller J, Dai Y, Andreasen JL, Hansen HN, De Chiffre L. Quantitative analysis of scaling error compensation methods in dimensional X-ray computed tomography. CIRP J Manuf Sci Technol 2015;10:68–76. https://doi.org/10.1016/j. cirpj.2015.04.004.
- [17] Dewulf W, Kiekens K, Tan Y, Welkenhuyzen F, Kruth JP. Uncertainty determination and quantification for dimensional measurements with industrial computed tomography. CIRP Ann. 2013;62(1):535–8. https://doi.org/10.1016/j. cirp.2013.03.017.
- [18] Lifton JJ, Malcolm AA, McBride JW. The application of voxel size correction in X-ray computed tomography for dimensional metrology. SG: 2nd Singapore International NDT Conference & Exhibition; 2013.
- [19] Ferrucci M, Hermánek P, Ametova E, Sbettega E, Vopalensky M, Kumpová I, et al. Measurement of the X-ray computed tomography instrument geometry by minimization of reprojection errors-Implementation on experimental data. Precis Eng 2018;54:107–17. https://doi.org/10.1016/j.precisioneng.2018.05.007.
- [20] Ferrucci M, Leach RK, Giusca C, Carmignato S, Dewulf W. Towards geometrical calibration of x-ray computed tomography systems-a review. Meas Sci Technol 2015;26(9). https://doi.org/10.1088/0957-0233/26/9/092003.
- [21] Neuschaefer-Rube U, Illemann J, Sturm M, Bircher BA, Meli F, Bellon C, et al. Validation of a fast and traceable radiographic scale calibration of dimensional computed tomography. Meas Sci Technol 2022;33(9). https://doi.org/10.1088/ 1361-6501/ac74a3.
- [22] Villarraga-Gómez H, Thousand JD, Smith ST. Empirical approaches to uncertainty analysis of X-ray computed tomography measurements: a review with examples. Precis Eng 2020;64:249–68. https://doi.org/10.1016/j.precisioneng.2020.03.004.